RSC Advances

PAPER

View Article Online
View Journal | View Issue

Crystal structure, topology, tiling and photoluminescence properties of 4d–4f hetero-metal organic frameworks based on 3,5-pyrazoledicaboxylate†

Cite this: *RSC Adv.*, 2014, **4**, 7818

Ting Hai Yang,[ab] Rute A. S. Ferreira,[c] Luis D. Carlos,[c] João Rocha[a] and Fa Nian Shi*[a]

Received 5th November 2013
Accepted 3rd January 2014

DOI: 10.1039/c3ra47686c

www.rsc.org/advances

Reaction of lanthanide oxides, cadmium acetate and 3,5-pyrazoledicarboxylic acid under hydrothermal conditions afforded five new isostructural 4d 4f hetero-metal organic frameworks, $[Cd_3Ln(pdc)_3(H_2O)]$ {H_3pdc 3,5-pyrazoledicarboxylic acid, Ln La (**1**), Pr (**2**), Nd (**3**), Sm (**4**) and Eu (**5**)}. All compounds were characterized by elemental analysis, infrared spectroscopy, thermogravimetric analysis, X-ray diffraction, scanning electron microscopy and energy dispersive X-ray spectroscopy. The compounds feature a very interesting 3D structure built up from a secondary building unit, $[Cd_{12}Ln_8(pdc)_6]$, and possess a new topology type and complicated unique tiling. The solid state photoluminescence properties of compounds **3–5** were investigated at room temperature.

Introduction

The design and construction of hetero-metal organic frameworks (HMOFs) attracts much attention due to their diverse and fascinating structures and potential applications in magnetism,[1] catalysis,[2] optoelectron,[3] and gas storage[4] *etc.* In the past two decades, much effort was devoted to the design of d–f hetero-metallic series.[5] However, most work has been focused on assembling 3d–4f systems, such as copper–lanthanide,[6] while 4d–4f HMOFs and their physical properties, particularly photoluminescence, remained poorly studied.[7] Therefore, the introduction of d^{10} Zn/Cd metals into the lanthanide–organic frameworks (LnOFs) may pave the way to new luminescent materials.[5g,h,8]

On the basis of the hard-and-soft-acid-base theory, it seems feasible to use N/O mixed ligands for synthesizing d–f HMOFs. The Ln ions prefer O-donors to N-donors, while d-block metal ions have a strong tendency to coordinate to both N- and O-donors. In this context, 3,5-pyrazoledicarboxylic acid (H_3pdc) is a promising N/O mixed ligand for the construction of high-dimensionality HMOFs due to its excellent coordination behaviour derived from its unique molecular structure (Fig. S1†). Indeed, it possesses multiple coordination sites involving two pyrazole nitrogen and four carboxylate oxygen atoms. With three different abstractable hydrogen atoms, it is a good ligand for constructing pyrazole-bridged heterometal complexes.[9] The planar and hetero-aromatic dicarboxylates are sterically compact allowing metal–metal interactions through the π orbitals.[6m] Moreover, H_3pdc can hold metal atoms closer, as compared with other five-membered diaza ring systems.[6k,n,9] Recently, we have reported an unusual 3D inorganic sub-network Zn–Ln MOF system $[Zn_3Ln(pdc)_3(H_2O)]\cdot 0.125H_2O$,[9b] exhibiting the highest quantum yield reported for a non-fluorinated MOF and an unusual 3D inorganic sub-network structure.

Comparison of Zn(II) to Cd(II), they both have d^{10} full-filled electron orbit, the difference is that Zn(II) has $3d^{10}$ as outer shell while Cd(II) has $4d^{10}$ as outer shell. Accordingly, the Cd(II) ionic radium is larger than that of Zn(II) which leads to form the covalent bonds in different bond strength, bond lengths and bond angles with the same organic ligands.[10] As a consequence, even if the complexes formed by Cd(II) and Zn(II) with the same ligands and even having the same composition, they crystallize in the different structures.[10] specific to Cd–Ln and Zn–Ln HMOFs,[11,12] no study has been reported on comparing any photoluminescence. For the first time, the similar structures of the Cd–Ln-pdc and Zn–Ln-pdc systems were designed so that the study of the comparative photoluminescence becomes possible and meaningful.[9b] Generally, Cd/Zn introduced into LnOFs can dilute the concentration of rare earth ions and reduce the concentration quenching effect, thus is ultimately beneficial for the rare earth photoluminescence.[9b,11 13]

[a]*Department of Chemistry, CICECO, University of Aveiro, 3810 193 Aveiro, Portugal. E mail: fshi@ua.pt; Fax: +351 234370084; Tel: +351 234401520*

[b]*School of Chemistry & Environmental Engineering, Jiangsu University of Technology, Changzhou 23001, P R China*

[c]*Department of Physics, CICECO, University of Aveiro, 3810 193 Aveiro, Portugal*

† Electronic supplementary information (ESI) available: IR data, SEM, TGA, photoluminescences and single crystal structure tables. CCDC 968561 968565. For ESI and crystallographic data in CIF or other electronic format see DOI: 10.1039/c3ra47686c

For comparative purposes and assessing the effect of d^{10}-block metals on the photoluminescence properties of HMOFs, we have prepared five new related HMOFs, in which Cd ions are present instead of Zn ions. Thus, here, five new related 4d–4f HMOFs formulated as $[Cd_3Ln(pdc)_3(H_2O)]$ {Ln = La (**1**), Pr (**2**), Nd (**3**), Sm (**4**) and Eu (**5**)} are described. The tiling of 3-periodic nets is presented here for the first time. The photoluminescence properties of the Zn and Cd materials also present differences.

Experimental

Materials and methods

All the starting materials were of reagent quality and obtained from commercial sources without further purification. Elemental analyses for C, N and H were performed on a TruSpec 630-200-200 CNHS Analyser. FT-IR spectra were collected from KBr pellets (Aldrich 99%+, FT-IR grade) on a Mattson 7000 FT-IR spectrometer in a range of 4000–400 cm^{-1} at the resolution of 2 cm^{-1}. Thermogravimetric analyses (TGA) were carried out using a Shimadzu TGA 50 under air, from room temperature to *ca.* 700 °C, with a heating rate of 5 °C min^{-1}. Powder X-ray diffraction (PXRD) patterns were recorded at ambient temperature on a X'Pert MPD Philips diffractometer (Cu Kα X-radiation, λ = 1.54060 Å), equipped with a X'Celerator detector, a curved graphite-monochromated radiation and a flat-plate sample holder, in a Bragg–Brentano para-focusing optics configuration (40 kV, 50 mA). Scanning electron microscopy (SEM) and energy dispersive analysis of X-ray spectroscopy (EDS) were performed using a Hitachi S-4100 field emission gun tungsten filament instrument working at 25 kV. Samples were prepared by deposition on aluminium sample holders by carbon coating. The photoluminescence spectra in the visible and NIR spectral ranges were recorded at room temperature with a modular double grating excitation spectrofluorimeter with a TRIAX 320 emission monochromator (Fluorolog-3, Horiba Scientific) coupled to a R928 and H9170 Hamamatsu photomultipliers, respectively, using a front face acquisition mode. The excitation source was a 450 W Xe arc lamp. The emission spectra were corrected for detection and optical spectral response of the spectrofluorimeter and the excitation spectra were corrected for the spectral distribution of the lamp intensity using a photodiode reference detector. The emission decay curves in the visible and NIR spectral regions were measured with the setup described for the luminescence spectra using a pulsed Xe–Hg lamp (6 μs pulse at half width and 20–30 μs tail).

Synthesis of compounds

Compounds **1–5** were obtained under the same experimental conditions. In a general synthesis, a mixture of Ln_2O_3 (0.05 mmol, 0.0163 g), $Cd(CH_3CO_2)_2$ (0.30 mmol, 0.0800 g), and H_3pdc (0.30 mmol, 0.0522 g) in 15 mL H_2O, was kept in a Teflon-line autoclave at 170 °C for 3 days. After slow cooling to room temperature, the colorless block-like crystals were collected as a single phase, judged by the powder X-ray diffraction measurement. For **1**, yield: 0.0812 (85%). Anal. found (calcd in %) for $C_{15}H_5N_6O_{13}Cd_3La$: C, 18.96 (18.90); H, 0.56 (0.53); N, 8.89 (8.82). IR (KBr, cm^{-1}): 3455(br), 1614(s), 1588(s), 1555(s), 1528(s), 1406(m), 1374(s), 1359(s), 1297(w), 1219(w), 1053(m), 1017(w), 844(m), 838(m), 811(w), 781(m), 634(w), 577(m), 538(w), 428(w), 350(w).

For **2**, yield: 0.0806 (84%). Anal. found (calcd in %) for $C_{15}H_5N_6O_{13}Cd_3Pr$: C, 18.93 (18.86); H, 0.57 (0.53); N, 8.91 (8.80). IR (KBr, cm^{-1}): 3450(br), 1612(s), 1587(s), 1554(s), 1530(s), 1408(m), 1376(s), 1361(s), 1299(w), 1220(w), 1053(m), 1018(w), 845(m), 837(m), 811(w), 780(m), 635(w), 578(m), 538(w), 430(w), 351(w).

For **3**, yield: 0.0809 (84%). Anal. found (calcd in %) for $C_{15}H_5N_6O_{13}Cd_3Nd$: C, 18.86 (18.79); H, 0.58 (0.53); N, 8.86 (8.77). IR (KBr, cm^{-1}): 3462(br), 1613(s), 1588(s), 1555(s), 1531(s), 1409(m), 1377(s), 1362(s), 1299(w), 1220(w), 1054(m), 1018(w), 845(m), 837(m), 810(w), 780(m), 635(w), 579(m), 539(w), 429(w), 352(w).

For **4**, yield: 0.0816 (85%). Anal. found (calcd in %) for $C_{15}H_5N_6O_{13}Cd_3Sm$: C, 18.76 (18.67); H, 0.55 (0.52); N, 8.79 (8.71). IR (KBr, cm^{-1}): 3480(br), 1614(s), 1587(s), 1555(s), 1530(s), 1411(m), 1379(s), 1364(s), 1299(w), 1221(w), 1054(m), 1019(w), 845(m), 837(m), 811(w), 779(m), 635(w), 578(m), 539(w), 429(w), 353(w).

For **5**, yield: 0.0813 (84%). Anal. found (calcd in %) for $C_{15}H_5N_6O_{13}Cd_3Eu$: C, 18.72 (18.64); H, 0.57 (0.52); N, 8.80 (8.70). IR (KBr, cm^{-1}): 3458(br), 1612(s), 1588(s), 1555(s), 1530(s), 1412(m), 1379(s), 1364(s), 1300(w), 1223(w), 1055(m), 1019(w), 846(m), 837(m), 811(w), 779(m), 636(w), 579(m), 531(w), 431(w), 352(w).

X-ray crystallographic analysis

Single crystals with dimensions 0.04 × 0.04 × 0.04 mm for **1**, 0.18 × 0.16 × 0.12 mm for **2**, 0.12 × 0.08 × 0.06 mm for **3**, 0.12 × 0.08 × 0.06 mm for **4** and 0.18 × 0.18 × 0.18 mm for **5** were selected for indexing and intensity date collection at 298 K on a Bruker SMART APEX-II CCD diffractometer equipped with graphite-monochromatized Mo Kα (λ = 0.71073 Å) radiation. A hemisphere of date was collected in the θ range 2.09–30.51° for **1**, 2.10–30.49° for **2**, 2.10–30.51° for **3**, 2.11–30.47° for **4** and 3.65–33.09° for **5** using a narrow-frame method with scan widths of 0.30°in ω and an exposure time of 10 s per frame. Numbers of measured and observed reflections [$I > 2\sigma(I)$] are 10 247 and 2439 (R_{int} = 0.0690) for **1**, 10 206 and 2388 (R_{int} = 0.0606) for **2**, 10 180, 2401 (R_{int} = 0.0682) for **3**, 10 074 and 2394 (R_{int} = 0.0671) for **4** and 13 823 and 2934 (R_{int} = 0.0275) for **5** respectively. The data were integrated using the Siemens SAINT program,[14] with the intensities corrected for Lorentz factor, polarization, air absorption, and absorption due to variation in the path length through the detector faceplate. The structures were solved by direct method using SHELXS and refined on F^2 by full matrix least-squares using SHELXL.[15] All the non-hydrogen atoms were refined anisotropically. All H atoms were refined isotropically. Crystallographic and refinement details are listed in Table 1. Selected bond lengths and bond angles are given in Table S1.† CCDC reference numbers: 968561–968565 correspond to (**1**), (**2**), (**3**), (**4**) and (**5**), respectively.

Table 1 Crystallographic data for compounds **1–5**

Compounds	**1**	**2**	**3**	**4**	**5**
Empirical formula	$C_{15}H_5N_6O_{13}Cd_3La$	$C_{15}H_5N_6O_{13}Cd_3Pr$	$C_{15}H_5N_6O_{13}Cd_3Nd$	$C_{15}H_5N_6O_{13}Cd_3Sm$	$C_{15}H_5N_6O_{13}Cd_3Eu$
F_w	953.36	955.36	958.69	964.68	966.41
Crystal system	Cubic	Cubic	Cubic	Cubic	Cubic
Space group	$Pa\bar{3}$	$Pa\bar{3}$	$Pa\bar{3}$	$Pa\bar{3}$	$Pa\bar{3}$
a b c (Å)	16.8954(13)	16.8075(4)	16.77180(10)	16.7466(2)	16.7360(2)
α β γ (°)	90	90	90	90	90
V (Å^3)	4792.1(6)	4748.0(2)	4717.79(5)	4696.56(10)	4687.65(10)
Z	8	8	8	8	8
D_c (g cm ^{3})	2.643	2.673	2.699	2.729	2.739
F(000)	3536	3552	3560	3576	3584
GOF on F^2	1.001	1.000	1.004	1.001	1.004
R_1, w$R_2{}^a$ [$I > 2\sigma(I)$]	0.0402, 0.0860	0.0359, 0.0590	0.0391, 0.0765	0.0392, 0.0534	0.0243, 0.0497
R_1, w$R_2{}^a$ (all date)	0.0700, 0.1031	0.0623, 0.0648	0.0553, 0.0815	0.0570, 0.0560	0.0344, 0.0518
$(\Delta\rho)_{max}$, $(\Delta\rho)_{min}$ (eÅ^3)	1.112, 1.083	2.091, 1.106	1.652, 1.009	3.371, 2.258	1.709, 1.163

^{a} R_1 $\Sigma||F_o|$ $|F_c||/\Sigma|F_o|$, wR_2 $[\Sigma w(F_o{}^2$ $F_c{}^2)^2/\Sigma w(F_o{}^2)^2]^{1/2}$.

Results and discussion

Description of structures

Compounds **1–5** are isostructural, and crystallize in the cubic lattice with $Pa\bar{3}$ space group. Hence, only the structure of **1** will be discussed in detail. The asymmetric unit consists of a one-third La atom, one Cd atom, one pdc^{3-} fragment and a one-third coordinated water molecule. As shown in Fig. 1, the Cd atom is in a distorted octahedral environment, surrounded by four oxygen atoms [O(1), O(2A), O(3C), O(4F)] and two nitrogen atoms [N(1) and N(2F)] from four equivalent pdc^{3-} fragments. The Cd–O bond lengths range from 2.181(5) to 2.6294 Å and the Cd–N bond lengths vary from 2.1835(2) to 2.2675 Å. The La atom is ten coordinated by nine oxygen atoms [O(1), O(1A), O(1B), O(3C), O(4C), O(3D), O(4D), O(3E), O(4E)] from six equivalent pdc^{3-} fragments and one coordinated water molecule [O(5)]. The La–O bonds lengths are in the range 2.593(4)–2.600(4) Å, comparable to those reported for compounds such as $[Ln_2Cd_2(p\text{-toluylate})_{10}(phen)_2]$, $[LnCd(imdc)(SO_4)(H_2O)_3]\cdot 0.5H_2O$, $[Ln_2Cd_3(EDTA)_3(H_2O)_{11}](H_2O)_{14}$, $[Cd_3Ln_2(btc)_4(H_2O)_6(dmf)_4]$, $[LnCd_2(imdc)_2(Ac)(H_2O)\cdot H_2O$, $\{[Ln_2(ODA)_6Cd_3(H_2O)_6]\cdot 6H_2O\}_n$.[8e j]

The H_3pdc carboxylate groups are completely deprotonated, as confirmed by the absence of an IR band at *ca.* 1701 cm^{-1}. The pdc^{3-} anion serves as a nine-dentate ligand, chelating one La atom and two Cd atoms and bridging one more La and two Cd atoms, respectively, in a μ_9-η^2N, O, η^2N′, O′, η^2O″, O″, η^1O‴, η^1O⁗, η^1O⁗⁗ fashion (Fig. S2†).

Each La atom is further surrounded by six Cd atoms, while each Cd atom is connected by two La atoms *via* the bridging oxygen atoms (Fig. 2). The shortest and longest distances between neighbouring La atoms is, respectively, 8.4590(8) and 11.4567(7) Å. If only the La atom is taken as a node, each La atom is surrounded by six other La atoms *via* a O···Cd···O bridge (Fig. S3†). Consequently, a 3D MOF is constructed, in which the secondary building unit (SBU), $[Cd_{12}Ln_8(pdc)_6]$

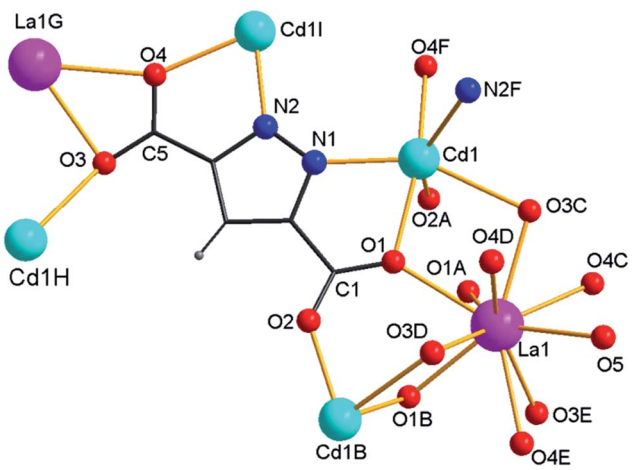

Fig. 1 The coordination environment of the Cd^{2+} and La^{3+} ions and the coordination mode of the pdc^3 ligand in **1**. All H atoms attached to water molecules are omitted for clarity. Symmetry codes are given in Table 1.

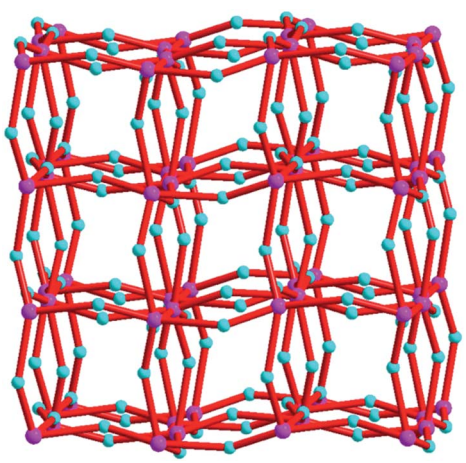

Fig. 2 Simplified inorganic framework structure of **1** with all C, N, O, and H atoms omitted. Pink ball: lanthanide atom; cyan ball: cadmium atom.

(Fig. 3), consists of six pdc^{3-} ligands extending on six faces of a cube, linking the neighboring ligands *via* metal nodes (12 Cd and 8 La atoms), and forming a hollow cuboidal sphere, with a diameter of 0.82 nm and a volume of *ca.* 288.69 $Å^3$.

The framework structure of **1** may be simplified using a topological approach. Each crystallographically independent metal centre is taken as a node, with intermetal bridges ensured by the bridging ligand. Each Cd^{2+} ions is connected to four pdc^{3-} ligands, and is viewed as a 4-connected node. Each La atom, in turn, is connected to six pdc^{3-} ligands, and is considered a 6-connected node. The pdc^{3-} ligand connects four Cd^{2+} and two La^{3+} ions and is viewed as a 6-connected node. On the basis of the topology analysis carried out with the TOPOS 4.0 programme,[16] structure **1** may be represented as a 4,6,6-connected net with the total point symbol $\{4^3.6^3\}_3\{4^3.6^9.8^3\}_3\{4^9.6^6\}$ (Fig. 4a). This topology type (we deposit it as fnc2 in TTD database)[17] has been found only in the Zn analogues.[9b]

Further analysis of the structure with TOPOS indicated that there are many rings formed *via* the metal atoms (Ln and/or Cd) and the ligand fragments (pdc^{3-}), ranging from 4-member and 6-member rings to 8-member rings, but none are self-catenated or catenated with other rings. A rare feature, 2-threading, occurs in one 8-member ring (Fig. 4b).[18]

Because the topology is new and the structure is high symmetry (cubic, $Pa\bar{3}$), it is of interest to analyse the tiling of the nets.[19] Indeed this tiling of the 3-periodic nets is rather complicated as revealed by the TOPOS, Systre and 3dt programmes.[16,20] Only one natural tiling (NT) and five primitive proper tilings (PPT, Fig. 5) are confirmed unprecedented in the RCSR database.[19b] The tiling figure was drawn with programme 3dt.

There are five kinds of tiles in NT (Fig. 5a) corresponding to 6 $[4.6^2]$, 6$[6^3]$, 2$[6^4]$, $[4^6.6^6]$ and $[4^{12}.6^8]$ with 3, 6, 7 and 5 of the inequivalent vertices, edges, faces and tiles (represented in 5 different colours). Three kinds of tiles were found in PPT1 (Fig. 5b): 6$[4^3.6^2]$, $[4^6.6^6]$ and $[6^{18}]$ with 3, 6, 5 and 3 inequivalent vertices, edges, faces and tiles in the tiling, respectively. A primitive proper tiling (PPT2, Fig. 5c) is with four kinds of tiles:

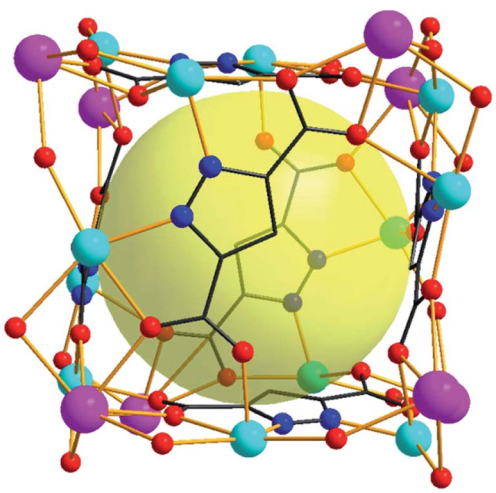

Fig. 3 Structure of the secondary building unit $[Cd_{12}Ln_8(pdc)_6]$. The yellow sphere depicts a hollow cage with a diameter of 0.82 nm.

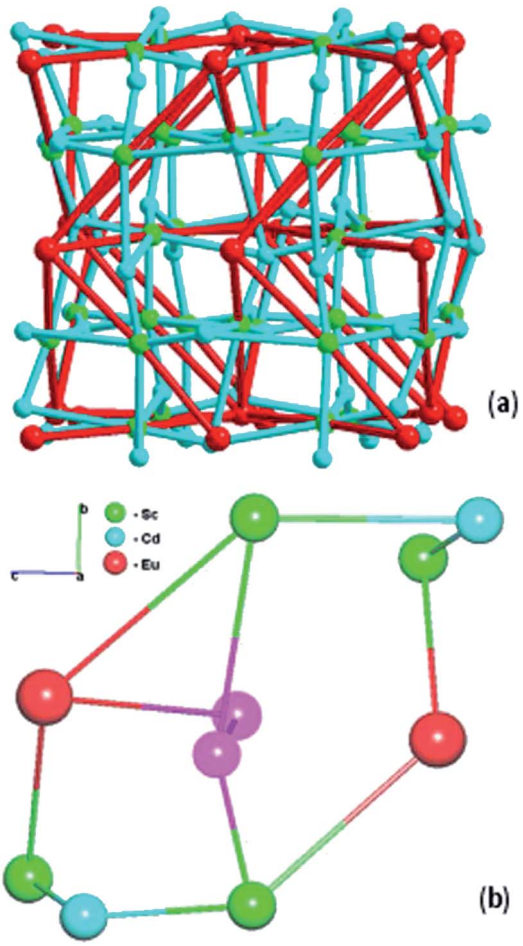

Fig. 4 (a) The topology structure of **1**; (b) 8-member ring with 2-threading. Red ball: lanthanide; cyan ball: cadmium atom; green ball: centre of gravity of pdc^3 ; pink ball: threading atoms.

6$[4.6^2]$, 6$[4.6^3]$, $[6^6]$ and $[4^{12}.6^{12}]$. There are 3, 6, 6 and 4 inequivalent vertices, edges, faces and tiles in the tiling, respectively. A primitive proper tiling (PPT3, Fig. 5d) has three kinds of tiles: 6$[4.6^4]$, $[4^6.6^6]$ and $[6^{18}]$ with 3, 6, 5 and 3 of the inequivalent vertices, edges, faces and tiles in the tiling, respectively. A primitive proper tiling (PPT4, Fig. 5e) has four kinds of tiles: 2 $[6^4]$, 2$[6^7]$, $[6^{14}]$ and $[6^{20}]$ with 3, 6, 6 and 4 inequivalent vertices, edges, faces and tiles in the tiling, respectively. A primitive proper tiling (PPT5, Fig. 5f) possesses four kinds of tiles: 2$[6^4]$, 2 $[6^7]$, 3$[6^8]$ and $[6^{14}]$ with 3, 6, 7 and 5 inequivalent vertices, edges, faces and tiles in the tiling, respectively. The duallized tilings for examples are selected to display in Fig. 6. The dualized NT (Fig. 6a) contains only 3 nonequivalent tiles: $[4^3.6^3]$, 3 $[4^2.6^3.8]$ and 3$[4.6^2.8]$, while the dualized PPT1 (Fig. 6b) has 3 different tiles: $[3^6]$, 3$[3^3.5.6^2]$ and 3$[3.5.6^2]$. They both reflect the cubic framework showing its high-symmetry nature.

Structures **2–5** are identical to **1** except for the different Ln ions. The shortest and longest Ln···Ln distances are: **2** (Pr) – 8.4393(4) and 11.3771(4) Å; **3** (Nd) 8.4225(4) and 11.3454(4) Å; **4** (Sm) – 8.4145(4) and 11.2995(4) Å; **5** (Eu) – 8.4124(2) Å and 11.2737(2) Å. The Ln–O bond lengths and unit-cell parameters decrease gradually from **1** to **5**, due to the lanthanide contraction.

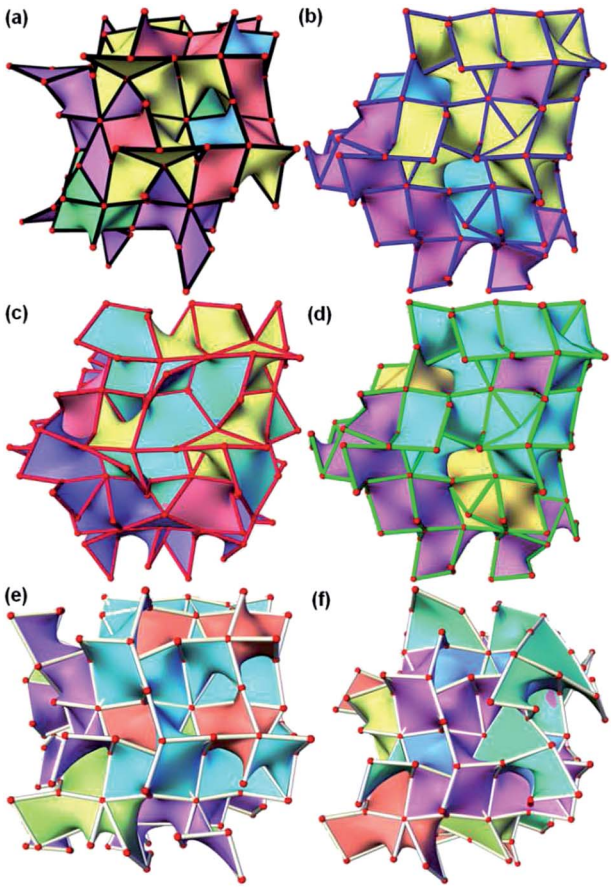

Fig. 5 The simple tilings of 3-periodic nets in **1**. (a) A natural tiling (NT). (b) A primitive proper tiling (PPT1). (c) A primitive proper tiling (PPT2). (d) A primitive proper tiling (PPT3). (e) A primitive proper tiling (PPT4). (f) A primitive proper tiling (PPT5). All viewed along the *X* axis.

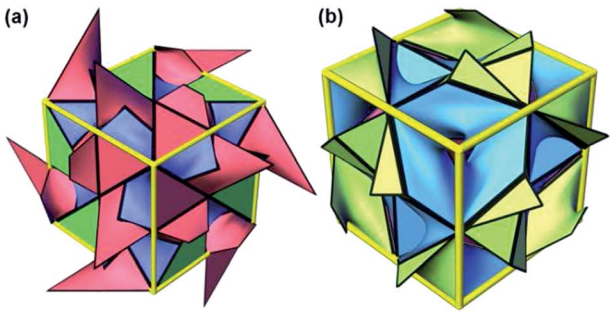

Fig. 6 (a) Dualized tiling of NT view along (111) plane shows the cubic framework, the yellow straight lines are the edges of the unit cell. (b) Dualized tiling of PPT 1 viewed along (111) plane, the thick yellow lines represent the edges of the unit cell.

Synthesis and IR spectra

Compounds **1–5** were synthesized under similar conditions using lanthanide oxides, cadmium acetate and 3,5-pyrazoledicarboxylic acid. For gadolinium and lutetium pure compounds could not be prepared.

The presence in **1–5** of coordination water molecules is indicated by a broad IR band of medium intensity at 3450–3480 cm^{-1}, assigned to ν(OH). No strong absorption peaks ranging from 1690 to 1730 cm^{-1} for –COOH are observed, confirming that all carboxyl groups of the H_3pdc ligand are deprotonated. The strong peaks at 1612–1359 cm^{-1} are assigned to the asymmetric and symmetric vibrations of the coordinated carboxylate groups (Fig. S4–S8†).

SEM and EDS

Scanning electron microscopy (SEM, Fig. 7 and S9†) shows particles with an almost homogeneous size distribution and similar crystal habits for all compounds. EDS analysis gave molar ratios Cd : La = 3 : 1 for (**1**), Cd : Pr = 3 : 1 for (**2**) Cd : Nd = 3 : 1 for (**3**), Cd : Sm = 3 : 1 for (**4**) and Cd : Eu = 3 : 1 for (**5**), in good agreement with the molecular formulae derived from the single crystal structures.

PXRD and thermal stability

Fig. 8 shows a good agreement between the experimental and simulated powder X-ray diffraction (PXRD) patterns of **1–5**, indicating the phase purity of the bulk products. The differences in reflection intensities are probably due to the preferred orientation effects. Thermal analyses were carried out for **1–5** to examine the thermal stabilities of these complexes (Fig. S10†). The thermogravimetry curves of **1–5** display similar thermal behaviours and good thermal stability (up to 400 °C) in air, presumably due to the framework stabilization of the 3D Ln–O–Cd subnetwork. The weight loss above 400 °C is due to the decomposition of the compounds and the collapse of the lattice. The final residue was not characterized.

Photoluminescence properties

Fig. 9a shows the emission spectra of **3**, **4** and **5**. Compounds **4** and **5** emit in the visible range a series of sharp lines assigned to the Sm^{3+} $^4G_{5/2} \rightarrow {}^6H_{5/2-11/2}$ transitions and Eu^{3+} $^5D_0 \rightarrow {}^7F_{0-4}$ transitions. Compound **3** emits in the near-infrared spectral range due to the Nd^{3+} $^4F_{3/2} \rightarrow {}^4I_{11/2,13/2}$ transitions. Because **1** gives a broad band in the blue/green spectral region due to the

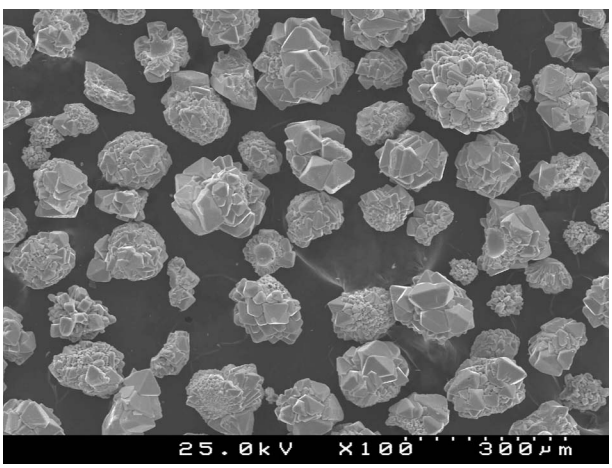

Fig. 7 SEM image of **1** showing aggregated particles.

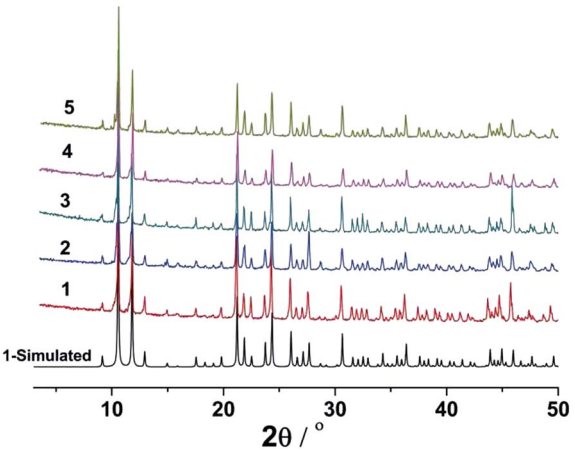

Fig. 8 Experimental and simulated PXRD patterns of **1–5**.

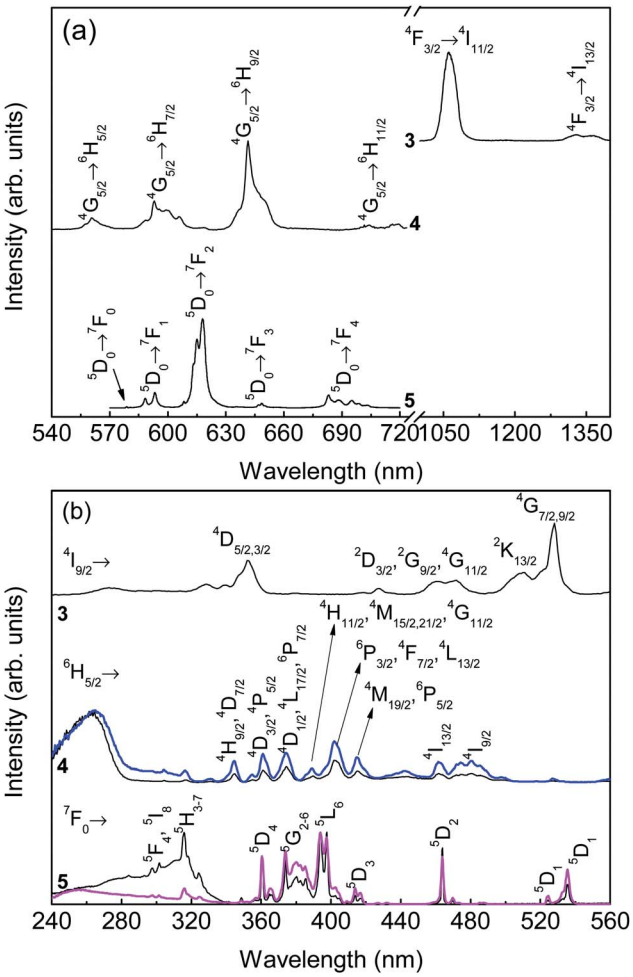

Fig. 9 (a) Emission and (b) excitation spectra of compounds **3**, **4** and **5** excited at 352 nm (**3**), 375 nm (**4**) and 320 nm (**5**) and monitored at 1062 nm (**3**), 642 nm (**4**) and 618 nm (**5**), respectively. The excitation spectra of the analogous Zn Ln MOF system $[Zn_3Ln(pdc)_3(H_2O)]\cdot 0.125H_2O$, with Ln Eu (magenta) and Ln Sm (blue) are also shown.[9b]

organic ligands, the absence of such emission component in Fig. 9a points out an effective ligands-to-Ln^{3+} (Ln = Nd, Sm and Eu) energy transfer. In all cases, the intra-4f emission is independent of the excitation wavelength (Fig. S11–S13, ESI†) in accord with the XRD data that show the Ln^{3+} ions occupy the same average local environment.

Fig. 9b compares the excitation spectra of compounds **3**, **4** and **5** monitored around the maximum emission peak position. For compounds **3** and **4**, the spectra consist of a broad band in the UV region with a main component at *ca.* 265 nm and a shoulder at 283 nm, respectively, ascribed to the pdc organic ligands excited states, as also detected for the inorganic subnetwork Zn–Ln MOF system $[Zn_3Ln(pdc)_3(H_2O)]\cdot 0.125H_2O$.[9b] For compound **5**, another component at *ca.* 315 nm is also present, resembling that observed for the $[Zn_3Eu(pdc)_3(H_2O)]\cdot 0.125H_2O$, being assigned to a ligand-to-Eu^{3+}-charge transfer (LMCT) band.[9b] We should note however, a significant increase in the relative intensity of the LMCT band in the presence of Cd atoms relatively to that found for the Zn-based MOF.[9b] All the excitation spectra also reveal a series of sharp lines ascribed to the intra-4f transitions typical of the Ln^{3+} ions. Comparing the relative intensity between these intra-4f lines and the pdc-related band, we note that only for compound **4** the relative intensity of the band is higher than that of the intra-4f lines. Therefore, the Sm^{3+} ions are mainly excited through the ligands rather than by direct intra-4f excitation, as observed for the Sm^{3+}- and Eu^{3+}-MOFs, $[Zn_3Ln(pdc)_3(H_2O)]\cdot 0.125H_2O$.[9b] For compounds **3** and **5**, the intra-4f lines are the most intense, meaning that direct intra-4f excitation is the main path for the population of the Nd^{3+} and Eu^{3+} ions.

The $^4I_{9/2}$ (Nd^{3+}), $^4G_{5/2}$ (Sm^{3+}) and $^5D_0$ (Eu^{3+}) emission decay curves were monitored around the maximum intensity peak position under direct excitation into the intra-4f levels (Fig. S14–S16, ESI†). All the curves are well described by a single exponential function, in good agreement with the presence of a single average Ln^{3+} local environment within each compound. From the fit to the emission decay curves, the lifetime values of the $^4I_{9/2}$, $^4G_{5/2}$ and of the $^5D_0$ excited states are 0.075 ± 0.001, 0.020 ± 0.001 and 0.511 ± 0.001, respectively. These values are higher than those measured for the analogous Zn–Ln MOF system $[Zn_3Ln(pdc)_3(H_2O)]\cdot 0.125H_2O$.[9b]

In order to rationalise this result, the $^5D_0$ radiative (k_r) and nonradiative (k_{nr}) transition probabilities and the $^5D_0$ quantum efficiency (η), $\eta = k_r/(k_r + k_{nr})$, using a procedure based on the $^5D_0 \rightarrow {}^7F_{0-4}$ integrated areas and $^5D_0$ lifetime (t), recorded at room temperature for the same excitation wavelength (395 nm) were calculated.[9b,21] The calculated k_r, k_{nr} and η values are 0.8 ms^{-1}, 1.2 ms^{-1} and 0.41, respectively. Comparing these values with those found for the Zn–Eu MOF,[9b] the k_r value is the same whereas it is observed a decrease in the k_{nr} therefore yielding a higher η value. The number of water molecules (n_w) coordinated to Eu^{3+} ions is determined using the empirical formula of Supkowski and Horrocks, $n_w = 1.11 \times [(k_{exp}\quad k_r\quad 0.31)]$, where k_{exp} is the experimental transition probability ($k_{exp} = \tau^{-1}$), yielding $n_w = 0.9 \pm 0.1$, in accord with the crystal structure (Eu^{3+} containing 1 coordinate water molecule). The differences on the non-radiative decay rates between Zn–Eu and Cd–Eu MOFs may be the consequence of the distinction of the first coordination

shell of Ln^{3+} in Zn–Ln MOFs and Cd–Ln MOFs. Although Ln^{3+} possess the same coordination number (CN = 10) in the two systems, the bond lengths Ln–O and angles of O–Ln–O are different in Zn–Ln MOFs[9b] and Cd–Ln MOFs (Table S1 in ESI†) and also with the alterations in the second neighborhood (obvious difference of Zn–O bonds and Cd–O bonds) as revealed by the single crystal structural data.

Conclusions

Five new 4d–4f hetero-metal organic frameworks formulated as $[Cd_3Ln(pdc)_3(H_2O)]$ { Ln = La (**1**), Pr (**2**), Nd (**3**), Sm (**4**), Eu (**5**)} were synthesized hydrothermally using lanthanide oxides, cadmium acetate and 3,5-pyrazoledicarboxylic acid. The compounds feature an interesting 3D framework constructed from the secondary building unit $[Cd_{12}Ln_8(pdc)_6]$ and a rare fnc2 topology type. The solid state emission and excitation spectra of compounds **3**, **4** and **5**, the lifetime of the $^4I_{9/2}$ (Nd^{3+}), $^4G_{5/2}$ (Sm^{3+}) and $^5D_0$ (Eu^{3+}) excited states as well as the $^5D_0$ quantum efficiency (η) of the Cd–Eu MOF are investigated in detail comparing to the analogues of Zn–Ln MOFs. In general, the lifetime of **3–5** and the $^5D_0$ quantum efficiency ($\eta = 0.41$) of **5** are higher than the analogues of Zn–Ln MOFs ($\eta = 0.33$).[9b]

Acknowledgements

We thank Fundação para a Ciência e a Tecnologia (FCT), FEDER, QREN, COMPETE (PEst-C/CTM/LA0011/2013) and (FCT: SFRH/BPD/74582/2010) for financial support. F.-N. SHI acknowledges FCT for PTDC/CTM-NAN/119994/2010. T.-H. Yang acknowledges the Natural Scientific Foundation for Universities in Jiangsu Province (13KJB150013) and the Science and Technology Bureau of Changzhou City (Project no. CJ20110014).

Notes and references

1 (*a*) C. Benelli and D. Gatteschi, *Chem. Rev.*, 2002, **102**, 2369; (*b*) J. Dreiser, K. S. Pedersen, C. Piamonteze, S. Rusponi, Z. Salman, M. E. Ali, M. Schau-Magnussen, C. A. Thuesen, S. Piligkos, H. Weihe, H. Mutka, O. Waldmann, P. Oppeneer, J. Bendix, F. Nolting and H. Brune, *Chem. Sci.*, 2012, **3**, 1024; (*c*) H. L. Gao, L. Yi, B. Ding, H. S. Wang, P. Cheng, D. Z. Liao and S. P. Yan, *Inorg. Chem.*, 2006, **45**, 481.

2 (*a*) M. Shibasaki and N. Yoshikawa, *Chem. Rev.*, 2002, **102**, 2187; (*b*) C. E. Plecnik, S. M. Liu and S. G. Shore, *Acc. Chem. Res.*, 2003, **36**, 499.

3 (*a*) M. Sakamoto, K. Manseki and H. Okawa, *Coord. Chem. Rev.*, 2001, **219**, 379; (*b*) B. Zhao, H. L. Gao, X. Y. Chen, P. Cheng, W. Shi, D. Z. Liao, S. P. Yan and Z. H. Jiang, *Chem. – Eur. J.*, 2006, **12**, 149; (*c*) B. D. Chandler, D. T. Cramb and G. K. H. Shimizu, *J. Am. Chem. Soc.*, 2006, **128**, 10403; (*d*) J. Niu, S. Zhang, H. Chen, J. Zhao, P. Ma and J. Wang, *Cryst. Growth Des.*, 2011, **11**, 3769.

4 (*a*) Y. Wang, P. Cheng, J. Chen, D.-Z. Liao and S.-P. Yan, *Inorg. Chem.*, 2007, **46**, 4530; (*b*) Z. Pan, J. Xu, H. Zheng, K. Huang, Y. Li, Z. Guo and S. R. Batten, *Inorg. Chem.*, 2009, **48**, 5772.

5 (*a*) J.-B. Peng, Q.-C. Zhang, X.-J. Kong, Y.-Z. Zheng, Y.-P. Ren, L.-S. Long, R.-B. Huang, L.-S. Zheng and Z. Zheng, *J. Am. Chem. Soc.*, 2012, **134**, 3314; (*b*) J.-B. Peng, Q.-C. Zhang, X.-J. Kong, Y.-P. Ren, L.-S. Long, R.-B. Huang, L.-S. Zheng and Z. Zheng, *Angew. Chem., Int. Ed.*, 2011, **50**, 10649; (*c*) R. Feng, L. Chen, Q.-H. Chen, X.-C. Shan, Y.-L. Gai, F.-L. Jiang and M.-C. Hong, *Cryst. Growth Des.*, 2011, **11**, 1705; (*d*) J. Rinck, G. Novitchi, W. Van den Heuvel, L. Ungur, Y. Lan, W. Wernsdorfer, C. E. Anson, L. F. Chibotaru and A. K. Powell, *Angew. Chem., Int. Ed.*, 2010, **49**, 7583; (*e*) Q. Zhang, Y.-X. Zheng, C.-X. Liu, Y.-G. Sun and E. J. Gao, *Inorg. Chem. Commun.*, 2009, **12**, 523; (*f*) T. K. Prasad, M. V. Rajasekharan and J.-P. Costes, *Angew. Chem., Int. Ed.*, 2007, **46**, 2851; (*g*) W. G. Lu, L. Jiang, X. L. Feng and T. B. Lu, *Cryst. Growth Des.*, 2006, **6**, 564; (*h*) L. Huebner, A. Kornienko, T. J. Emge and J. G. Brennan, *Inorg. Chem.*, 2004, **43**, 5659; (*i*) G. M. Li, T. Akitsu, O. Sato and Y. Einaga, *J. Am. Chem. Soc.*, 2003, **125**, 12396.

6 (*a*) Q.-B. Bo, G.-X. Sun and D.-L. Geng, *Inorg. Chem.*, 2010, **49**, 561; (*b*) A. M. Madalan, N. Avarvari, M. Fourmigue, R. Clerac, L. F. Chibotaru, S. Clima and M. Andruh, *Inorg. Chem.*, 2008, **47**, 940; (*c*) S. Xiang, S. Hu, T. Sheng, R. Fu, X. Wu and X. Zhang, *J. Am. Chem. Soc.*, 2007, **129**, 15144; (*d*) J. W. Cheng, J. Zhang, S. T. Zheng, M. B. Zhang and G. Y. Yang, *Angew. Chem., Int. Ed.*, 2006, **45**, 73; (*e*) C. Aronica, G. Pilet, G. Chastanet, W. Wernsdorfer, J.-F. Jacquot and D. Luneau, *Angew. Chem., Int. Ed.*, 2006, **45**, 4659; (*f*) M. B. Zhang, J. Zhang, S. T. Zheng and G. Y. Yang, *Angew. Chem., Int. Ed.*, 2005, **44**, 1385; (*g*) S. M. Liu, C. E. Plecnik, E. A. Meyers and S. G. Shore, *Inorg. Chem.*, 2005, **44**, 282; (*h*) Y. P. Cai, C. Y. Su, G. B. Li, Z. W. Mao, C. Zhang, A. W. Xu and B. S. Kang, *Inorg. Chim. Acta*, 2005, **358**, 1298; (*i*) Y. P. Cai, G. B. Li, Q. G. Zhan, F. Sun, J. G. Zhang, S. Gao and A. W. Xu, *J. Solid State Chem.*, 2005, **178**, 3729; (*j*) J. P. Costes, J. M. Clemente-Juan, F. Dahan and J. Milon, *Inorg. Chem.*, 2004, **43**, 8200; (*k*) Y. M. Chen, L. N. Zheng, S. X. She, Z. Chen, B. Hu and Y. H. Li, *Dalton Trans.*, 2011, **40**, 4970; (*l*) X. H. Zhou, Y. H. Peng, Z. G. Gu, J. L. Zuo and X. Z. You, *Inorg. Chim. Acta*, 2009, **362**, 3447; (*m*) X. H. Zhou, Y. H. Peng, X. D. Du, C. F. Wang, J. L. Zuo and X. Z. You, *Cryst. Growth Des.*, 2009, **9**, 1028; (*n*) Y. Wang, Y. Song, Z. R. Pan, Y. Z. Shen, Z. Hu, Z. J. Guo and H. G. Zheng, *Dalton Trans.*, 2008, 5588.

7 (*a*) L.-Q. Fan, Y. Chen, J.-H. Wu and Y.-F. Huang, *J. Solid State Chem.*, 2011, **184**, 899; (*b*) Y.-P. Cai, X.-X. Zhou, Z.-Y. Zhou, S.-Z. Zhu, P. K. Thallapally and J. Liu, *Inorg. Chem.*, 2009, **48**, 6341; (*c*) Y.-P. Cai, Q.-Y. Yu, Z.-Y. Zhou, Z.-J. Hu, H.-C. Fang, N. Wang, Q.-G. Zhan, L. Chen and C.-Y. Su, *CrystEngComm*, 2009, **11**, 1006; (*d*) B. Zhao, X. Q. Zhao, Z. Chen, W. Shi, P. Cheng, S. P. Yan and D. Z. Liao, *CrystEngComm*, 2008, **10**, 1144; (*e*) Y.-G. Sun, X.-M. Yan, F. Ding, E.-J. Gao, W.-Z. Zhang and F. Verpoort, *Inorg. Chem. Commun.*, 2008, **11**, 1117; (*f*) Y. C. Liang, R. Cao, W. P. Su and M. C. Hong, *Chem. Lett.*, 2000, 868.

8 (*a*) X. Q. Zhao, B. Zhao, W. Shi, P. Cheng, D. Z. Liao and S. P. Yan, *Dalton Trans.*, 2009, 2281; (*b*) Y. X. Chi, S. Y. Niu, Z. L. Wang and J. Jin, *Chem. J. Chin. Univ.*, 2008, **29**, 1081; (*c*) T. K. Prasad and M. V. Rajasekharan, *Cryst. Growth Des.*, 2008, **8**, 1346; (*d*) Y. X. Chi, S. Y. Niu, Z. L. Wang and J. Jin, *Eur. J. Inorg. Chem.*, 2008, 2336; (*e*) Y. X. Chi, S. Y. Niu, J. Jin, R. Wang and Y. Li, *Dalton Trans.*, 2009, 7653; (*f*) Y. Q. Sun, J. Zhang and G. Y. Yang, *Chem. Commun.*, 2006, 4700; (*g*) Q. Liu, S. Z. Ge, J. C. Zhong, Y. Q. Sun and Y. P. Chen, *Dalton Trans.*, 2013, **42**, 6314; (*h*) H. Yang, F. Wang, Y. X. Tian, Y. Kang, T. H. Li and J. Zhang, *Chem. – Asian J.*, 2012, **7**, 1069; (*i*) A. Ablet, S. M. Li, W. Cao, X. J. Zheng, W. T. Wong and L. P. Jin, *Chem. – Asian J.*, 2013, **8**, 95; (*j*) J. X. Ma, X. F. Huang, X. Q. Song and W. S. Liu, *Chem. – Eur. J.*, 2013, **19**, 3590; (*k*) S. M. T. Abtab, A. Audhya, N. Kundu, S. K. Samanta, P. S. Sardar, R. J. Buthcher, S. Ghosh and M. Chaudhury, *Dalton Trans.*, 2013, **42**, 1848; (*l*) S. L. Cai, S. R. Zheng, Z. Z. Wen, J. Fan and W. G. Zhang, *Cryst. Growth Des.*, 2012, **12**, 5737.

9 (*a*) V. Chandrasekhar and R. Thirumoorthi, *Organometallics*, 2009, **28**, 2096; (*b*) C. B. Liu, R. A. S. Ferreira, F. A. A. Paz, A. Cadiau, L. D. Carlos, L. S. Fu, J. Rocha and F. N. Shi, *Chem. Commun.*, 2012, **48**, 7964; (*c*) F. N. Shi, A. R. Silva, T. H. Yang and J. Rocha, *CrystEngComm*, 2013, **15**, 3776; (*d*) T. H. Yang, A. R. Silva and F. N. Shi, *Dalton Trans.*, 2013, **42**, 13997.

10 S. M. T. Abtab, A. Audhya, N. Kundu, S. K. Samanta, P. S. Sardar, R. J. Butcher, S. Ghoshb and M. Chaudhury, *Dalton Trans.*, 2013, **42**, 1848.

11 X. Yang, D. Schipper, R. A. Jones, L. A. Lytwak, B. J. Holliday and S. Huang, *J. Am. Chem. Soc.*, 2013, **135**, 8468.

12 (*a*) S.-M. Li, X.-J. Zheng, D.-Q. Yuan, A. Ablet and L.-P. Jin, *Inorg. Chem.*, 2012, **51**, 1201; (*b*) X. Feng, L.-F. Ma, L. Liu, L.-Y. Wang, H.-L. Song and S.-Y. Xie, *Cryst. Growth Des.*, 2013, **13**, 4469; (*c*) X. Feng, Y.-Q. Feng, L. Liu, L.-Y. Wang, H.-L. Song and S.-W. Ngd, *Dalton Trans.*, 2013, **42**, 7741.

13 F.-N. Shi, M. L. Pinto, D. Ananias and J. Rocha, *Microporous Mesoporous Mater.*, 2014, DOI: 10.1016/j.micromeso.2014.01.012.

14 SAINT+, *Data Integration Engine, v. 7.23a*, Bruker AXS, Madison, Wisconsin, 1997–2005.

15 G. M. Sheldrick, *Acta Crystallogr., Sect. A: Found. Crystallogr.*, 2008, **64**, 112.

16 (*a*) V. A. Blatov and A. P. Shevchenko, *TOPOS – Version Professional beta evaluation*, Samara State University, Samara, Russia, 2006; (*b*) V. A. Blatov, A. P. Shevchenko and V. N. Serezhkin, *J. Appl. Crystallogr.*, 2000, **33**, 1193.

17 V. A. Blatov and A. P. Shevchenko, *TOPOS–TTD database*, Samara State University, Samara, Russia, updated September, 2013.

18 Z. G. Gu, X. X. Xu, W. Zhou, C. Y. Pang, F. F. Bao and Z. J. Li, *Chem. Commun.*, 2012, **48**, 3212.

19 (*a*) O. Delgado-Friedrichs, M. O'Keeffe and O. M. Yaghi, *Phys. Chem. Chem. Phys.*, 2007, **9**, 1035; (*b*) M. O'Keeffe, M. A. Peskov, S. J. Ramsden and O. M. Yaghi, *Acc. Chem. Res.*, 2008, **41**, 1782.

20 Olaf Delgado-Friedrichs, Systre and 3dt, programs are free available on line:http://gavrog.org/.

21 L. D. Carlos, R. A. S. Ferreira, V. de Zea Bermudez and S. J. L. Ribeiro, *Adv. Mater.*, 2009, **21**, 509–534.